Acta Crystallographica Section B
Structural Science
ISSN 0108-7681

The modulated structure of $Ba_{0.39}Sr_{0.61}Nb_2O_6$. I. Harmonic solution

Theo Woike,[a]* Václav Petříček,[b] Michal Dušek,[b] Niels K. Hansen,[c] Pierre Fertey,[c] Claude Lecomte,[c] Alla Arakcheeva,[d] Gervais Chapuis,[d] Mirco Imlau[e] and Rainer Pankrath[e]

[a]Institut für Mineralogie, Universität zu Köln, Zülpicher Strasse 49, D-50674 Köln, Germany, [b]Institute of Physics, Academy of Sciences of the Czech Republic, Na Slovance 2, 182 21 Praha 8, Czech Republic, [c]Laboratoire de Cristallographie et Modélisation des Matériaux Minéraux et Biologique, Univeristé Henri Poincaré, BP 239, 54506 Vandoeuvre-lès-Nancy CEDEX, France, [d]Université de Lausanne, Institut de Crystallographie, BSP Dorigny, CH-1015 Lausanne, Switzerland, and [e]Fachbereich Physik, Universität Osnabrück, Barbarastrasse 7, D-49069 Osnabrück, Germany

Correspondence e-mail: th.woike@uni-koeln.de

Received 12 August 2002
Accepted 20 November 2002

The structure of a crystal of $Sr_{0.61}Ba_{0.39}Nb_2O_6$ has been solved and refined as an incommensurate structure in five-dimensional superspace. The structure is tetragonal, superspace group $P4bm(pp1/2, p-p1/2)$, unit-cell parameters $a = 12.4566$ (9), $c = 7.8698$ (6) Å, modulation vectors $\mathbf{q}_1 = 0.3075$ (6) ($\mathbf{a}^* + \mathbf{b}^*$), $\mathbf{q}_2 = 0.3075$ (6) ($\mathbf{a}^* - \mathbf{b}^*$). The data collection was performed on a KUMA-CCD diffractometer and allowed the integration of weak first-order satellite reflections. The structure was refined from 2569 reflections to a final value of $R = 0.0479$. The modulation affects mainly the positions of the O atoms, which are displaced by as much as 0.5 Å, and the site 4*c* that is occupied by Sr and Ba atoms. Only a simplified model, in which this atomic position is occupied by an effective atom Sr/Ba, could be refined from the data set. The modulation of displacement parameters has been used to account for the modulated distribution of Sr and Ba. The whole refinement uses only first-order modulation waves, but there are strong indications that for a complete solution the use of higher-order satellites and a more complicated model is necessary.

1. Introduction

$Sr_{1-x}Ba_xNb_2O_3$ (SBN-100[$1-x$]), $0.25 < x < 0.75$, is a very attractive material for technological applications and basic research because of the large pyroelectric, electrooptic and piezoelectric tensor components (Lines & Glass, 1977; Ewbank *et al.*, 1987; Neurgaonkar *et al.*, 1981). This material is of special interest in the fields of holographic data storage (Qiao *et al.*, 1993) and relaxor-type phase transitions. The key feature of relaxor ferroelectrics is that they have low-frequency polydispersive polar dynamics, which result in a temperature and frequency dependence of the dielectric permitivity [this feature was discovered by Smolenskii; see Smolenskii & Agranovskaya (1958)]. The order parameter (the ferroelectric polarization) is smeared out over a broad temperature range, and the ammount of the linear tensor components increases and reaches a broad maximum. If the material is heated to just above the maximum temperature of the phase transition no significant loss of the polarization can be detected (Granzow *et al.*, 2002) by macroscopic methods, *e.g.* pyroelectricity. However, it has been shown that SBN has a critical phase-transition temperature T_c, and some critical exponents are determined by evaluating the temperature dependence of the birefringence (Lehnen *et al.*, 2000) or NMR measurements (Blinc *et al.*, 2001). On the basis of these results Lehnen *et al.* (2001) have proposed a random-field Ising model to explain the relaxor behaviour of SBN.

It is, therefore, of special interest to analyse the contribution of the structural disorder to the phase-transition behaviour. Since SBN belongs to the disordered tetragonal unfilled

tungsten-bronze family with the non-centrosymmetric point group 4*mm* in the ferro-phase and 4/*mmm* in the para-phase, the tetragonal symmetry is conserved and the mirror plane perpendicular to the fourfold axis is lost at the phase transition. For undoped SBN the maximum of the phase-transition temperature lies in the range 353–358 K. Of course, the shift of the permitivity peak with increasing frequency cannot be explained by structural disorder, but the structural disorder should affect the origin of the random field. The frequency shift is bound to the domain dynamic and domain clustering.

The structure of SBN crystals has already been the subject of numerous investigations since the pioneering work of Jamieson *et al.* (1968) on SBN-73. They used the space group *P*4*bm*, which is in accordance with the ferroelectric properties of the crystal. Nevertheless, deviations of atomic positions from those in the centrosymmetric space group *P*4/*mbm* are highly significant (about 0.106 Å for Nb2) but relatively small. The idealized structure with the generalized formula $A_2B_4C_4Nb_2Nb_8O_{30}$ is presented in Fig. 1. The Nb—O octahedra are linked by corners and form three different kinds of cavities. The first 12-fold-coordinated cavity *A* (2*a* site) is either empty or occupied by Sr. The second 15-fold-coordinated cavity *B* (4*c* site) is empty or occupied by Ba or Sr. The position *B* is always partly empty, hence the name 'unfilled tungsten-bronze structure'. The small ninefold-coordinated cavity *C* (4*c* site) is always empty. Thus the five Sr and Ba ions are distributed over six positions on two different sites *A* and *B*. The O ions in the Ba and Sr layer (O4 and O5) are disordered, as is obvious from the shape of their thermal ellipsoids and the Fourier maps. In Jamieson's original work O4 and O5 were refined as split atoms. Similar results were later obtained by Andreichuk *et al.* (1984) for SBN-33 and in the most recent work by Chernaya *et al.* (1997) for SBN-61. By doping SBN with Ce or Cr, the *B* position is occupied by Ce in an off-centre position and Cr is incorporated into the Nb position (Woike *et al.*, 1997, 2001; Wingbermühle *et al.*, 2000).

Later Schneck *et al.* (1981) found for SBN-71 satellite spots at $h \pm (1+\delta)/4$, $k \pm (1+\delta)/4$, $l + 1/2$, where $\delta = 0.26$ (5). This result revealed the incommensurate character of the crystal, which is similar to the previously discovered incommensurability in $Ba_2NaNb_5O_{15}$ (BNN) (Schneck & Denoyer, 1981). Belagurov *et al.* (1987) confirmed these results using the neutron time-of-flight method and the triple-axis technique for crystals with $x = 0.3$. Another neutron time-of-flight measurement by Prokert *et al.* (1991) showed that the modulation parameter δ slightly decreases with increasing x for different compositions, $0.46 < x < 0.75$, and with low doping concentrations of Nd and Mn. HRTEM (high-resolution transmission electron microscope) and electron diffraction studies were performed by Bursill & Lin (1986, 1987). From these studies and from the supercell model of BNN, Lin & Bursill (1987) have built a model of SBN by analogy. The superspace approach, as introduced into the structure analysis of modulated crystals by de Wolff (1974) and de Wolff *et al.* (1981), has not yet been introduced. This approach should give a more realistic description of the incommensurate structure of SBN. The purpose of the present paper is to perform such an analysis on the data set obtained from a modern CCD diffractometer, which gives higher-precision intensities of satellite reflections. The congruent melting composition $Sr_{0.61}Ba_{0.39}Nb_2O_6$, *i.e.* SBN-61, has been chosen for the present study.

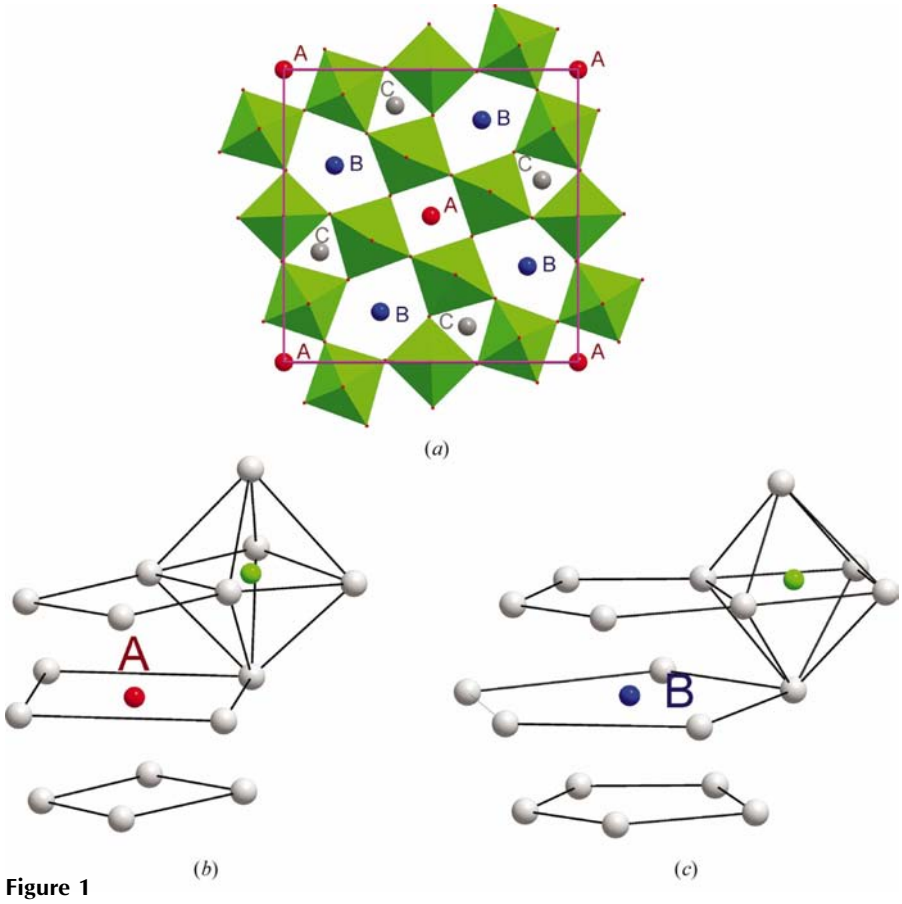

Figure 1
The average structure of SBN: (*a*) view on (001) face, (*b*) 12-fold-coordinated cavity of type *A*, (*c*) 15-fold-coordinated cavity of type *B*.

2. Experimental

Preliminary X-ray investigations from a Nonius CCD diffractometer revealed a diffraction pattern similar to those previously described (Schneck *et al.*, 1981). The data were collected on a KUMA-CCD four-circle diffractometer using the *KM*4*CCD* software (KUMA Diffraction, 2000). The modulation is two-dimensional, with modulation vectors $\mathbf{q}_1 = \alpha(\mathbf{a}^* + \mathbf{b}^*) + 1/2\mathbf{c}^*$ and $\mathbf{q}_2 = \alpha(\mathbf{a}^* - \mathbf{b}^*) + 1/2\mathbf{c}^*$, where $\mathbf{a}^*$, $\mathbf{b}^*$ and $\mathbf{c}^*$ are the reciprocal axes of the basic

Table 1
Experimental details.

Crystal data	
Chemical formula	$Ba_{0.39}Nb_2O_6Sr_{0.61}$
Chemical formula weight	388.81
Cell setting, superspace group	Tetragonal, $X4bm(pp0, p-p0)$
Non-primitive translation	(0, 0, 1/2, 1/2, 1/2)
a, c (Å)	12.4566 (9), 7.8698 (6)
V (Å^3)	1221.13 (16)
Z	10
D_x (Mg m^{-3})	5.286 (1)
D_m (Mg m^{-3})	5.286 (3)
Modulation wavevectors	$\mathbf{q}_1 = 0.3075\ (6)\ (\mathbf{a}^* + \mathbf{b}^*)$ $\mathbf{q}_2 = 0.3075\ (6)\ (\mathbf{a}^* - \mathbf{b}^*)$
Data collection	
Radiation type	Mo $K\alpha$
No. of reflections for cell parameters	594
θ range (°)	6.5–26.8
μ (mm^{-1})	14.31
Temperature (K)	293
Crystal form, colour	Sphere, colourless
Crystal radius (mm)	0.13
Diffractometer	KUMA CCD
Data collection method	ω scan, integration method
Absorption correction	Analytical
T_{min}	0.058
T_{max}	0.088
No. of measured, independent and observed parameters	27797, 5214, 2569
No. of main reflections	1021
No. of satellite reflections	1548
Criterion for observed reflections	$I > 3\sigma(I)$
R_{int}	0.08
θ_{max}	32
Range of h, k, l, m, n	$-18 \Rightarrow h \Rightarrow 18$ $-16 \Rightarrow k \Rightarrow 18$ $-11 \Rightarrow l \Rightarrow 11$ $-1 \Rightarrow m \Rightarrow 1$ $-1 \Rightarrow n \Rightarrow 1$
Intensity decay (%)	<3%
Refinement	
Refinement on	F
$R[F^2 > 2\sigma(F^2)]$, $wR(F^2)$, S	0.048, 0.058, 2.82
R, wR (main reflections)	0.033, 0.045
R, wR (satellites)	0.121, 0.126
No. of relections and parameters used in refinement	2569, 130
Weighting scheme	$w = 1/[\sigma^2(F) + 0.000025F^2]$
$(\Delta/\sigma)_{max}$	0.041
$\Delta\rho_{max}$, $\Delta\rho_{min}$ (e Å^{-3})	3.39, −4.67
Extinction method	B-C type 1 Lorentzian isotropic (Becker & Coppens, 1974)
Min. extinction transmission factor	0.615
Source of atomic scattering factors	*International Tables for X-ray Crystallography* (1992, Vol. C)
Extinction coefficient	0.289379

† Computer programs used: *JANA*2000 (Petricek & Dusek, 2000).

structure. The coefficient $\alpha = 0.3075\ (6)$ was determined by the least-squares method from 156 satellites. The refined α value corresponds to $\delta = 0.230\ (2)$, which is in accordance with the value found by Schneck *et al.* (1981).

All reflections observed on the collected frames were indexed by five integers $hklmn$ with respect to the five-dimensional base $\mathbf{h} = h\mathbf{a}^* + k\mathbf{b}^* + l\mathbf{c}^* + m\mathbf{q}_1 + n\mathbf{q}_2$ (de Wolff, 1974). The integration of main reflections ($hkl00$) and first-order satellites ($hkl10$), ($hkl01$) was performed with the *KUMA* software (KUMA Diffraction, 2000). Mixed satellites ($hkl11$), $(hkl1\bar{1})$ could not be integrated as they were located too close to main reflections. Data were corrected for Lorentz and polarization factors and for absorption.

All single crystals were grown by the Czochralski method. The composition and purity were checked by X-ray fluorescence and by neutron-activation analysis (Woike *et al.*, 1997, 2001) and was found to be Sr = 0.611 (2), Ba = 0.388 (2), Nb = 2.005 (5). The result showed a very high quality and purity of the studied congruent crystals. The density measured with large single crystals by the flotation method, $D_m = 5.286\ (3)$ Mg m^{-3}, is in a good agreement with the density calculated from cell parameters under the assumption of the congruent composition $D_x = 5.2856\ (7)$ Mg m^{-3}. Table 1 shows the experimental details.[1]

3. Structure determination

3.1. Refinement of the average structure

The positional parameters from the refinement made by Chernaya *et al.* (1997) SBN-61 were used to start the refinement of the average structure. The refinement quickly converged to $R = 0.0359$ for 1021 main reflections [$I > 3\sigma(I)$]. Atomic coordinates and equivalent isotropic displacement parameters for the average structure are given in Table 2. The basic features of the solution are consistent with those published by Jamieson *et al.* (1968) and Chernaya *et al.* (1997). The site 2*a* is only occupied by strontium and the site 4*c* is occupied by both barium and strontium. The refined occupancies lead to $x = 0.360\ (13)$, which is in reasonable accordance with the congruent composition.

The refined coordinates allow preliminary calculations based on bond-valence sums (Brese & O'Keeffe, 1991) of the present cations Ba and Sr, which should both be around two. The bond-valence sums calculated from the averaged distances at the 2*a* site are 2.230 (14) and 3.53 (2) for Sr and Ba, respectively. This result means that this site is too small to be occupied by a Ba atom unless a strong positional distortion is present. This site could have been a source of modulation in the crystal, but the fact that the site is exclusively occupied by Sr proves that the modulation does not arise from this site. On the other hand the bond-valence sums for the site 4*c* are 2.039 (15) and 1.281 (9) for Ba and Sr, respectively, which means that this site can be occupied alternately by both atoms. An ordered occupation of Sr and Ba could lead to a modulation in the crystal and it would also induce a positional modulation of the O atoms. This hypothesis is in accordance with the observed large atomic displacement parameters in the average structure as represented in Fig. 2 for O4 and O5 in the Ba and Sr layer.

[1] Supplementary data for this paper are available from the IUCr electronic archives (Reference: SN0027). Services for accessing these data are described at the back of the journal.

Table 2
Fractional atomic coordinates and equivalent isotropic displacement parameters (Å^2) for the average structure $B_{eq} = \sum_i \sum_j U_{ij} a_i^* a_j^* a_i a_j$.

Atom	Site occupancy	x	y	z	B_{eq}
Nb1	1	0	0.5	0.00268 (19)	0.00812 (16)
Nb2	1	0.07451 (3)	0.21161 (3)	−0.00708 (17)	0.00980 (13)
Sr1	0.71 (5)	0	0	0.2382 (2)	0.0064 (3)
Ba2/Sr2	0.450 (16) /0.442 (20)	0.17227 (3)	0.67227 (3)	0.24093	0.0255 (2)
O1	1	0.2179 (3)	0.2821 (3)	−0.0150 (15)	0.0204 (14)
O2	1	0.1389 (4)	0.0695 (3)	−0.0254 (11)	0.0316 (19)
O3	1	−0.0065 (4)	0.3441 (3)	−0.0229 (14)	0.035 (2)
O4	1	0	0.5	0.2340 (14)	0.067 (5)
O5	1	0.0838 (9)	0.2005 (6)	0.2299 (9)	0.057 (3)

3.2. Refinement of the modulated structure

The symmetry of the average structure suggests two possible superspace groups: $P4bm(pp1/2, p-p1/2)$ or $P4bm(pp1/2, p-p1/2)0gg$ (Yamamoto, 1996). The latter would lead to additional extinctions that were not confirmed from the data collection, and the former was therefore used for this study.

The third non-zero component of the modulation vectors is fixed by the symmetry. The non-zero part of the modulation vectors can be removed by doubling the lattice constant along the c direction (de Wolff *et al.*, 1981) with respect to the constant used in previous papers. This transformation leads to a complete separation of the external and internal space and simplifies the restrictions of the modulation parameters of the site symmetry. Thus the new five-dimensional cell has one non-primitive centring vector (0, 0, 1/2, 1/2, 1/2).

As a consequence of periodicity in the (3+2)-dimensional superspace, each parameter of the modulated structure can be expanded as a Fourier series,

$$p^{\mu}(x_4, x_5) = \sum_n \sum_m \left[p^{\mu}_{snm} \sin(2\pi n x_4 + 2\pi m x_5) + p^{\mu}_{cnm} \cos(2\pi n x_4 + 2\pi m x_5) \right], \quad (1)$$

where $x_4 = \mathbf{q}_1 \mathbf{r}^{\mu} + t$, $x_5 = \mathbf{q}_2 \mathbf{r}^{\mu} + u$, and t and u are internal phases. Only the terms $(nm) = (1, 0)$ and $(nm) = (0, 1)$ were used in the refinement because only first order satellites were collected.

The refinement of the positional modulation started from small displacements of the atoms, which converged smoothly to $R = 0.0658$, 0.0356 and 0.2171 for all, main and satellite reflections, respectively. A common modulation wave for Sr2/Ba2 atoms was applied at this stage. The consecutive difference-Fourier maps revealed large minima and maxima close to this position. In some regions, the distribution of both atoms around their common refined modulated position is more dispersed (Fig. 3*a*) while in other regions it is more concentrated (Fig. 3*b*). This result indicates that the simple positional modulation does not explain correctly the behaviour of Ba2 and Sr2 atoms and that some additional modulation needs to be introduced. The different distribution as a function of the internal coordinates can be caused by an occupational modulation and/or by a split of modulated positions of Ba2 and Sr2. Therefore a model that included the occupational modulation together with individual positional modulation for both atoms was proposed and refined. Unfortunately, strong correlations between the refined parameters led to an unstable refinement. The modulated atomic positions of Ba2 and Sr2 are so close together that the resolution does not allow them to be refined independently. This fact is in accordance with the observation made by Jamieson *et al.* (1968) that for SBN no clear site splitting was observed for Sr, Ba or Nb positions. Therefore, in the model

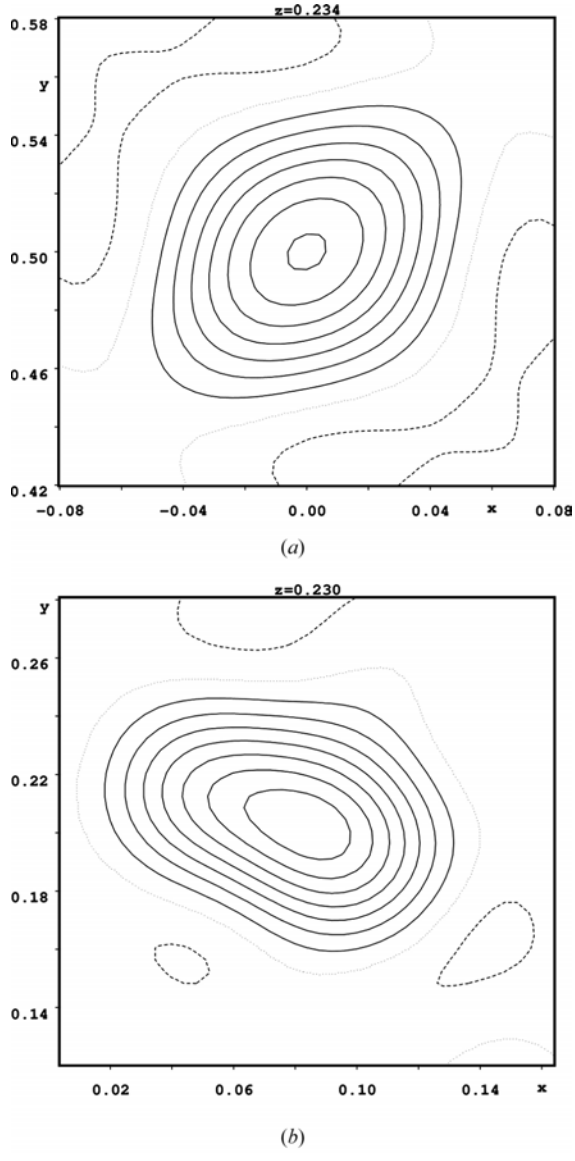

Figure 2
xy section of the electron density map based on normal Bragg reflections through the atomic position (*a*) at O4 and (*b*) at O5. Contour interval 1 e Å^{-3}.

used here, the effective centre Ba2/Sr2 has positional modulation and the additional distribution of Ba2/Sr2 atoms over this site is described as a modulation of atomic displacement parameters. This model converged to considerably lower values of $R = 0.0479$, 0.0334 and 0.1205. The refined positional parameters and refined atomic displacement parameters and their respective modulations are given in the supplementary material. Table 3 reports selected interatomic distances and angles together with bond-valence sums.

4. Discussion

As the crystal used for the structure determination was not poled we have refined the Flack's coefficient to account for the possible presence of both enantiomorphic domains. The refined value 0.486 (17) corresponds to the fact that both domains are equally occupied.

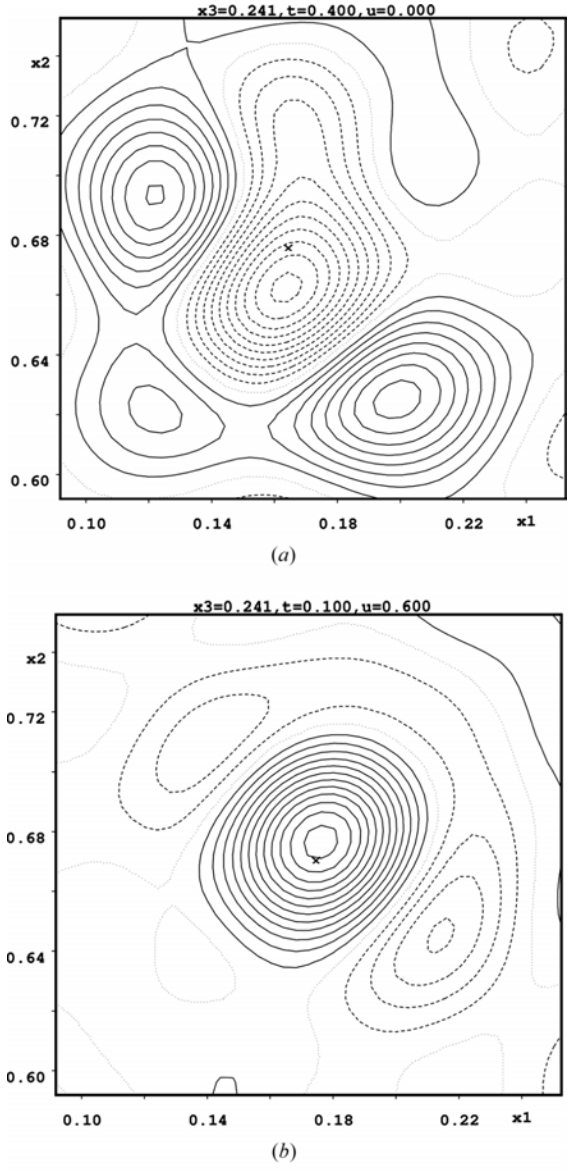

Figure 3
x_1–x_2 section of the electron density map through the atomic position of Sr2/Ba2 (*a*) at $t = 0.4$, $u = 0$ and (*b*) at $t = 0.1$, $u = 0.6$. Contour interval 1 e Å^{-3}.

Table 3
Interatomic distances (Å) and octahedral angles (°) in the modulated structure of $Ba_{039}Sr_{061}Nb_2O_6$.

	Average	Minimal	Maximal
Nb1—O octahedra			
Nb1—O3,O3^{i},O3^{ii},O3^{iii}	1.97 (2)	1.88 (2)	2.06 (2)
O3—Nb1—O3^{i}	167.5 (6)	166.1 (6)	169.3 (6)
O3—Nb1—O3^{ii}	93.6 (9)	86.4 (9)	100.6 (9)
O3—Nb1—O3^{iii}	85.3 (9)	76.5 (8)	92.7 (9)
O3—Nb1—O4	96.2 (7)	94.7 (7)	97.9 (7)
O3—Nb1—O4^{iv}	83.8 (6)	82.1 (6)	85.4 (6)
Nb1—O4	1.86 (3)	1.70 (6)	1.97 (6)
O4—Nb1—O4^{iv}	179.7 (6)	179.5 (6)	180
Nb1—O4^{iv}	2.13 (3)	1.97 (6)	2.23 (6)
O4^{iv}—Nb1—O4	179.7 (6)	179.5 (6)	180
Bond-valence sum	5.18 (18)	4.89 (16)	5.8 (3)
Nb2—O octahedra			
Nb2—O1	2.00 (2)	1.96 (2)	2.02 (2)
O1—Nb2—O2	91.1 (9)	83.6 (9)	99.4 (9)
O1—Nb2—O2^{v}	172.9 (6)	168.9 (6)	175.9 (6)
O1—Nb2—O3	94.9 (9)	90.2 (9)	98.8 (9)
O1—Nb2—O5	93.0 (6)	88.6 (6)	97.3 (6)
O1—Nb2—O5^{iv}	88.0 (6)	84.0 (5)	92.2 (6)
Nb2—O2	1.96 (2)	1.91 (2)	2.009 (18)
O2—Nb2—O2^{v}	88.4 (8)	78.3 (9)	96.6 (8)
O2—Nb2—O3	169.0 (7)	163.7 (8)	172.7 (6)
O2—Nb2—O5	91.4 (6)	90.1 (6)	93.0 (5)
O2—Nb2—O5^{iv}	82.8 (5)	81.2 (5)	84.3 (5)
Nb2—O2^{v}	2.03 (2)	1.97 (2)	2.072 (18)
O2^{v}—Nb2—O3	84.7 (8)	80.0 (8)	88.0 (8)
O2^{v}—Nb2—O5	93.6 (6)	92.8 (6)	94.1 (6)
O2^{v}—Nb2—O5^{iv}	85.3 (5)	84.7 (6)	86.3 (6)
Nb2—O3	1.95 (2)	1.90 (2)	2.00 (2)
O3—Nb2—O5	96.8 (6)	93.4 (6)	99.1 (6)
O3—Nb2—O5^{iv}	88.9 (6)	86.4 (5)	92.4 (6)
Nb2—O5	1.91 (3)	1.79 (3)	1.98 (3)
O5—Nb2—O5^{iv}	174.1 (5)	173.8 (5)	174.5 (5)
Nb2—O5^{iv}	2.09 (3)	1.95 (3)	2.18 (3)
Bond valence sum	4.94 (13)	4.39 (11)	5.71 (15)
Sr1—O polyhedra			
Sr1—O2,O2^{v},O2^{viii},O2^{x}	2.855 (17)	2.456 (17)	3.248 (16)
Sr1—O2^{vi},O2^{vii},O2^{ix},O2^{xi}	2.681 (18)	2.477 (19)	2.908 (17)
Sr1—O5,O5^{x},O5^{viii},O5^{x}	2.728 (12)	2.580 (13)	2.869 (12)
Bond valence sum	2.34 (3)	2.17 (3)	2.39 (4)
Sr2/Ba2—O polyhedra			
Sr2/Ba2—O1^{xii}	2.816 (18)	2.65 (2)	2.992 (19)
Sr2/Ba2—O1^{xiii}	2.722 (19)	2.57 (2)	2.894 (19)
Sr2/Ba2—O2^{xiii}	3.244 (19)	2.962 (18)	3.528 (17)
Sr2/Ba2—O2^{xv}	3.249 (19)	2.963 (18)	3.528 (17)
Sr2/Ba2—O3^{i}	2.943 (18)	2.618 (19)	3.293 (17)
Sr2/Ba2—O3^{xvi}	2.793 (19)	2.577 (19)	3.024 (18)
Sr2/Ba2—O3^{ii}	2.934 (18)	2.618 (19)	3.294 (17)
Sr2/Ba2—O3^{xvii}	2.786 (19)	2.576 (19)	3.024 (18)
Sr2/Ba2—O5^{xii}	3.169 (14)	2.532 (14)	3.785 (14)
Sr2/Ba2O5^{i}	3.455 (14)	2.803 (14)	4.126 (14)
Sr2/Ba2—O5^{ii}	3.487 (14)	2.803 (14)	4.126 (14)
Sr2/Ba2—O5^{xiv}	3.149 (14)	2.532 (14)	3.785 (14)
Sr2/Ba2—O4	3.045 (10)	2.693 (9)	3.366 (9)
Bond valence sum:			
Sr^{2+}	1.45 (2)	1.226 (16)	1.67 (3)
Ba^{2+}	2.30 (4)	1.95 (3)	2.67 (5)

† Symmetry codes: (i) $-x, 1-y, z$; (ii) $\frac{1}{2}-y, \frac{1}{2}-x, z$; (iii) $-\frac{1}{2}+y, \frac{1}{2}+x, \frac{1}{2}+z$; (iv) $x, y, -\frac{1}{2}+z$; (v) $-y, x, z$; (vi) $x, y, \frac{1}{2}+z$; (vii) $-y, x, \frac{1}{2}+z$; (viii) $-x, -y, z$; (ix) $-x, -y, \frac{1}{2}+z$; (x) $y, -x, z$; (xi) $y, -x, \frac{1}{2}+z$; (xii) $\frac{1}{2}-x, \frac{1}{2}+y, z$; (xiii) $\frac{1}{2}-x, \frac{1}{2}+y, \frac{1}{2}+z$; (xiv) $y, 1-x, z$; (xv) $y, 1-x, \frac{1}{2}+z$; (xvi) $-x, 1-y, \frac{1}{2}+z$; (xvii) $\frac{1}{2}-y, \frac{1}{2}-x, \frac{1}{2}+z$.

The positional modulation affects mainly O atoms, which are displaced by as much as 0.5 Å from their average positions. The low sensitivity of X-rays to O-atom modulations leads to relatively low intensities of satellite reflections, and therefore the standard uncertainties of the O-atom modulation parameters are large. This lack of sensitivity is also the origin of strong correlations between modulation parameters and average displacement parameters. For this reason only individual isotropic displacement parameters were refined for each O atom.

The positional modulation of the central atoms of the Nb octahedra is not very strong. The almost rigid octahedra are modulated mainly rotationally as predicted by Bursill & Lin (1987). Nevertheless the shape of Nb octahedra is also modulated, as can be seen from Fig. 4. The average Nb valences, as calculated by the bond-valence method given by Brese & O'Keeffe (1991), are equal within three standard uncertainties to 5; these values are in accordance with the formal valence of 5+. However, the minimal and maximal values are partly affected by possible anharmonicity in the modulation, as discussed below.

The Sr1 atom localized at 2*a* is almost modulation free. The attempt to refine its occupational modulation did not lead to significant improvement. Therefore the reduction of the occupancy by about 29% is not related to the observed modulation. The bond valence of this atom varies from 2.17 (3) to 2.39 (4). The positional modulation proposed by Bursill & Lin (1987) is based on different sequences of clockwise (*C*) and anticlockwise (*A*) displacements of O atoms. Such a modulation would make just a slight distortion of the square of O5 atoms that coordinate with the Sr1 position. However, in the present refinement the modulation of O5 atoms induces strong distortion of the square (see Fig. 5) as a result of continuous harmonic incommensurate modulation. Only a discontinuous modulation function, similar to the crenel function (Petříček *et al.*, 1995), could give a model composed only of *C* and *A* displacements. Such a modulation would lead to additional higher-order mixed satellites (*hkl*11), (*hkl*1 −1) and/or second-order (*hkl*20), (*hkl*02) satellites. Unfortunately the data set used for the refinement did not allow for the integration of higher-order satellites.

The 4*c* site is occupied partly by Sr and Ba. Moreover this site is not fully occupied either. The modulation of this position is rather complex. We have tested several split models but the data did not allow the Sr and Ba atoms to be refined individually. The best reasonably converging model uses a unique modulated position occupied by an effective atom that is composed of Sr and Ba. The modulation of anisotropic displacement parameters of this effective atom has been used to account for a modulated distribution of Sr and Ba atoms. The average occupancy of Sr1 was fixed to yield, together with the refined occupancies of Sr2 and Ba2, a sum corresponding to the general formula $Sr_{1-x}Ba_xNb_2O_6$. The refined values lead finally to $x = 0.40$ (2), which fits very well with the nominal congruent composition. The ellipsoids that describe anisotropic displacement are strongly modulated, as shown in Figs. 4 and 5. It is difficult to interpret these ellipsoids, as they describe a distribution of two atoms that have different diffraction powers. The longest principal axis of the displacement tensor is oriented mainly in the *xy* plane, and its length and direction are correlated with a distortion of the coordination pentagon of O atoms that lies at the same height as the central Sr2/Ba2 atom (see Fig. 4). The larger ellipsoids are located in the larger and more elongated pentagons. The refined average positions give bond-valence sums varying from 1.226 (16) to 1.67 (3) and from 1.95 (3) to 2.67 (5) for Sr^{2+} and Ba^{2+}, respectively.

The simple harmonic model refined in this paper was checked by special difference-Fourier maps at positions of the O atoms. The difference-Fourier map was based on the phases of all atoms except the O atom under inspection. This map was

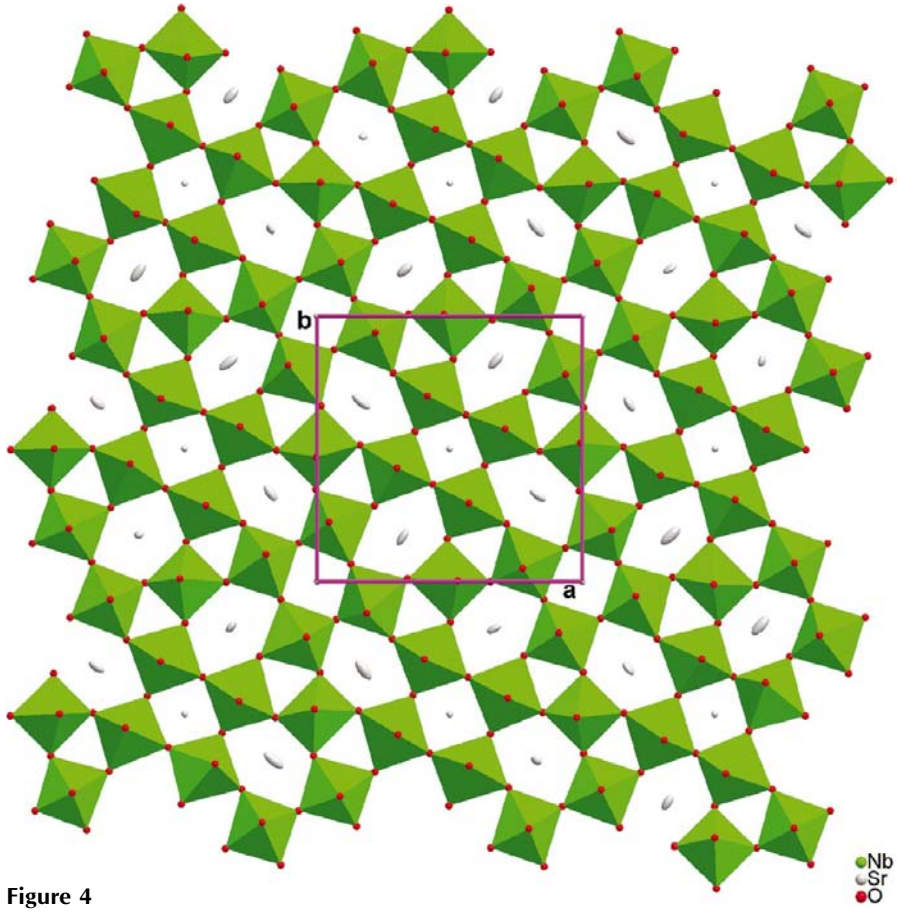

Figure 4
The Sr/Ba layer viewed along *c*. The modulation of anisotropic displacement parameters of Sr2/Ba2 is indicated by 70% probability displacement ellipsoids.

used instead of a regular Fourier map and was strongly affected by noise originating from peaks of the heavy atoms. According to (1), the harmonic model uses two waves that have arguments x_4 and x_5, respectively. Such a modulation function should have the same functional shape as a function of x_4 for any fixed value of x_5 and *vice versa*. The difference-Fourier maps (Fig. 6) indicate that the density has a more complicated shape. The amplitude of the modulation curve is clearly different for $x_5 = 0$ and $x_5 = 0.6$, which reinforces the necessity to add mixed modulation waves. We were not able to refine those additional amplitudes reliably because of the limitations imposed by the absence of higher-order satellites.

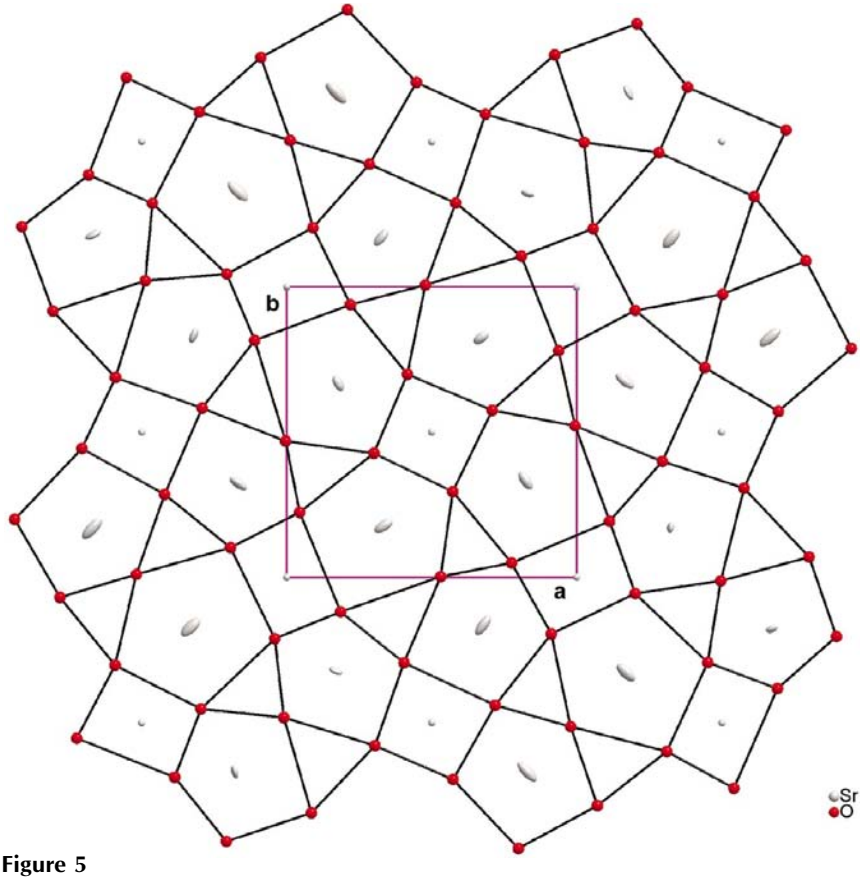

Figure 5
Projection of the structure of the Nb octahedra viewed along the *c* axis.

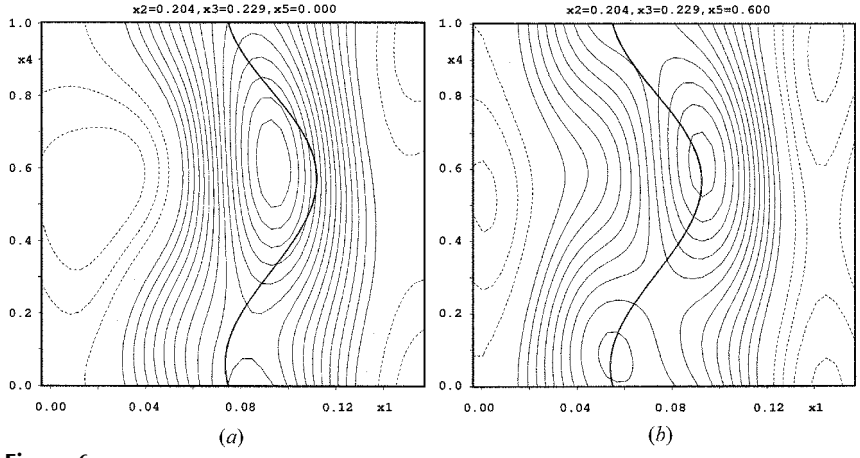

Figure 6
x_1–x_4 section of the electron density map through the atomic position of O5 (*a*) for $x_5 = 0$ and (*b*) for $x_5 = 0.6$.

5. Conclusion

The crystal structure analysis based on the superspace approach showed the main features of the modulation in the studied compound. The whole study is based on data collected with a KUMA-CCD diffractometer from which first-order satellites were successfully integrated. All previous attempts to collect data with point-detector diffractometers gave insufficient accuracy for satellites and the refinement could not be performed.

Previous diffraction studies of SBN were only concerned with its average atomic structure or speculated on the existence of a domain structure with an orthorhombic deformation of the parent tetragonal structure. The present study is the first successful attempt to describe SBN as a modulated tetragonal structure; the only domains taken into account correspond to the inversion of the ferroelectric polarization. Unfortunately this study cannot give a definitive description of all aspects of this structure. As shown in the discussion it is obvious that higher-order satellites are required for a more detailed solution. Such a new data collection cannot be performed on laboratory CCD diffractometers. Higher-intensity synchrotron radiation is necessary to record the stronger and sharper diffraction pattern that is required for integration of additional satellites.

This work was supported by the Deutsche Forschungsgemeinschaft (SPP 1056, Wo618/3-2) and by the Grant Agency of the Czech Republic (grant 202/03/0430). ThW and VP are very indebted to the LCM3B and the University Henry Poincare of Nancy for their stay as guest professors in Nancy during the main part of this work. AA gratefully acknowledges the Herbette Foundation of the University of Lausanne.

References

Andreichuk, A. E., Dorozhkin, L. M., Kuzminov, Yu. S., Maslyanitsyn, I. A., Molchanov, V. N., Rusakov, A. A., Simonov, V. I., Shigorin, V. D. & Shipulo, G. P. (1984). *Kristallografiya*, **20**, 1094–1101.
Becker, P. & Coppens, P. (1974). *Acta Cryst.* A**30**, 129–147.

Belagurov, A. M., Prokert, F. & Savenko, B. N. (1987). *Phys. Status Solidi A*, **103**, 131–144.
Blinc, R., Gregorovic, A., Zalar, R., Pirc, J., Seliger, S., Kleemann, W., Lushnikov, S. G. & Pankrath, R. (2001). *Phys. Rev. B*, **64**, 134109–134112.
Brese, N. E. & O'Keeffe, M. (1991). *Acta Cryst.* B**47**, 192–197.
Bursill, L. A. & Lin, P. J. (1986). *Philos. Mag. B*, **54**, 157–170.
Bursill, L. A. & Lin, P. J. (1987). *Acta Cryst.* B**43**, 49–56.
Chernaya, T. S., Maksimov, B. A., Verin, I. V., Ivleva, L. I. & Simonov, V. I. (1997). *Kristallografiya*, **42**, 421–426.
Ewbank, M. D., Neurgaonkar, R. R., Cory, W. K. & Feinberg, J. (1987). *J. Appl. Phys.* **62**, 374–379.
Granzow, T., Dörfler, U., Woike, Th., Wöhlecke, M., Pankrath, R., Imlau, M. & Kleemann, W. (2002). *Appl. Phys. Lett.* **80**, 470–472.
Jamieson, P. B., Abrahams, S. C. & Bernstein, J. L. (1968). *J. Chem. Phys.* **48**, 5048–5057.
KUMA Diffraction (2000). *KM4CCD System Software.* Version 1.162. Kuma Diffraction Instruments and Université de Lausanne, Switzerland.
Lehnen, P., Kleemann, W., Woike, Th. & Pankrath, R. (2000). *Eur. Phys. J. B*, **14**, 633–639.
Lehnen, P., Kleemann, W., Woike, Th. & Pankrath, R. (2001). *Phys. Rev. B*, **64**, 224109.
Lin, P. J. & Bursill, L. A. (1987). *Acta Cryst.* B**43**, 504–512.
Lines, M. E. & Glass, A. M. (1977). *Principles and Applications of Ferroelectrics and Related Materials.* Oxford: Clarendon Press.
Neurgaonkar, R. R., Cory, W. K., Ho, W. W., Hall, W. F. & Cross, L. E. (1981). *Ferroelectrics*, **38**, 857–861.
Petříček, V. & Dušek, M. (2000). *JANA*2000. *Programs for Modulated and Composite Crystals.* Institute of Physics, Praha, Czech Republic.
Petříček, V., van der Lee, A. & Evain, M. (1995). *Acta Cryst.* A**51**, 529–535.
Prokert, F., Sangaa, D. & Savenko, B. N. (1991). *Ferroelectr. Lett.* **13**, 61–66.
Qiao, Y., Orlov, S., Psaltis, D. & Neurgaonkar, R. R. (1993). *Opt. Lett.* **18**, 1004–1007.
Schneck, J. & Denoyer, F. (1981). *Phys. Rev. B*, **23**, 383–388.
Schneck, J., Toledano, J. C., Whatmore, R. & Ainger, F. W. (1981). *Ferroelectrics*, **36**, 327–330.
Smolenskii, G. A. & Agranovskaya, A. I. (1958). *Sov. Phys. Tech. Phys.* **3**, 1380–1389.
Wingbermühle, J., Meyer, M., Schirmer, O. F., Pankrath, R. & Kremer, A. K. (2000). *J. Phys. Condens. Matter*, **12**, 4277–4280.
Woike, Th., Dörfler, U., Tsankov, L., Weckwerth, G., Wolf, D., Wöhlecke, M., Granzow, T., Pankrath, R., Imlau, M. & Kleemann, W. (2001). *Appl. Phys.* B**72**, 661–666.
Woike, Th., Weckwerth, G., Palme, H. & Pankrath, R. (1997). *Solid State Commun.* **102**, 743–746.
Wolff, P. M. de (1974). *Acta Cryst.* A**30**, 777–785.
Wolff, P. M. de, Janssen, T. & Janner, A. (1981). *Acta Cryst.* A**37**, 625–636.
Yamamoto, A. (1996). *Acta Cryst.* A**52**, 509–560.